MicroRNA-29a contributes to intracranial aneurysm by regulating the mitochondrial apoptotic pathway

WENJING ZHAO[1], HAIFANG ZHANG[2] and JIN-YING SU[1]

[1]First Department of Neurology, Affiliated Hospital of Hebei University of Engineering, Handan, Hebei 056002; [2]Department of Cardiovascular Medicine, People's Hospital of Handan, Handan, Hebei 056001, P.R. China

Received April 12, 2017; Accepted February 16, 2018

DOI: 10.3892/mmr.2018.9257

Abstract. Intracranial aneurysm (IA) is an abnormal expansion in the intracranial arteries that weakens the arterial wall by consistently pushing the vascular wall outwards, which leads to a higher risk of aneurysm rupture. A number of reports have demonstrated that apoptosis is associated with the growth and rupture of IA. MicroRNAs (miRNAs/miRs) perform vital roles in the regulation of the mitochondrial apoptotic pathway and signaling proteins. Increasing evidence has already revealed the role of miR-29a in injury, including liver injury, cardiovascular injury and ischaemia-reperfusion injury. However, the role of miR-29a in IA remains unclear at present. The present study investigated the role of miR-29a in IA pathogenesis and the underlying mechanisms. By using reverse transcription-quantitative polymerase chain reaction and western blot analysis, the present study demonstrated that genes, including caspase-3, -8 and -9, and proteins, including cytochrome c and myeloid cell leukemia 1 (Mcl-1), involved in mitochondrial apoptosis pathways were upregulated in IA groups compared with controls. In addition, microarray analysis demonstrated that miR-29a, one of the most altered miRs in IA mice, was overexpressed in IA mice compared with controls. *In vitro* experiments revealed that miR-29a downregulation attenuated human brain vascular smooth muscle cell (HBVSMC) apoptosis, while miR-29a overexpression increased the apoptosis of HBVSMCs. Furthermore, luciferase reporter analysis revealed that Mcl-1 is a direct target gene of miR-29a. An *in vivo* IA model confirmed that miR-29a overexpression may promote apoptosis through mitochondrial pathways. It was therefore concluded that miR-29a may contribute to the progression of IA by regulating mitochondrial apoptotic pathways. Thus, miR-29a is a potential therapeutic target for IA.

Correspondence to: Professor Haifang Zhang, Department of Cardiovascular Medicine, People's Hospital of Handan, 49 Laodong Road, Handan, Hebei 056001, P.R. China
E-mail: haifangzhanghf@yeah.net

Key words: intracranial aneurysm, microRNA-29a, myeloid cell leukemia 1, mitochondrial apoptotic pathways

Introduction

Intracranial aneurysm (IA) is an abnormal expansion in the intracranial arteries that weakens the arterial wall by consistently pushing the vascular wall outwards, which leads to a risk of aneurysm rupture (1,2). It occurs in 2-3% of humans worldwide (3,4). Although treatment and prevention options exist, the majority of vascular remodeling cases lead to eventual rupture (5). At present, various molecular mechanisms have been demonstrated to be involved in the pathophysiology of IA, including cellular apoptosis (6,7).

Apoptosis, an energy-dependent form of cell death, occurs in a number of physiological conditions, including tissue remodeling, cell viability and cancer regression (8,9). Studies have been conducted concerning the involvement of apoptosis in IA growth and rupture (7,10). Pentimalli *et al* (7) revealed that aneurysm rupture is frequently associated with elevated levels of apoptosis, which may serve an essential role in weakening aneurysm walls, thereby resulting in dilation and rupture. By using rabbits as animal models, Kadirvel *et al* (11) reported that intrinsic pathway apoptosis occurred in aneurysms induced by elastase. However, few studies have been published concerning the apoptosis events in IA mice, and the underlying molecular mechanisms are yet to be established.

MicroRNAs (miRNAs/miRs) are a group of small (18-22 nucleotides) noncoding RNAs that negatively regulate gene expression either via inhibiting translation or inducing the degradation of target mRNAs (12), which allows them to exhibit regulatory effects on various genes, pathways and complex biological networks in cells. At present, a wide range of miRNAs have been identified in mice, rat and human cells, and studies have identified numerous roles for miRNAs in normal cell homeostasis and disease (13-15). Certain miRNAs function physiologically in the cardiovascular system (16-18). For example, miR-9 has been reported to contribute IA development by inhibiting proliferation and weakening the contractility of smooth muscle cells (19), while miR-133 is reported to serve as the key regulator in the phenotypic shift of vascular smooth muscle cells (VSMCs) *in vivo* and *in vitro* (20). In addition, miR-145 has been reported to be downregulated in atherosclerosis, vascular injury and aneurysms (21,22). Recently, evidence has emerged that demonstrates that certain specific miRNAs may serve a vital role in the development of IA (23,24). However, the role of miR-29a in the apoptosis

process associated with IA, and the underlying mechanisms, remain to be elucidated.

The present study therefore used an experimental IA model and demonstrated that miR-29a is able to regulate mitochondrial apoptosis, which contributes to the process of IA.

Materials and methods

Initiation of experimental IA. To induce cerebral aneurysms, male wild-type mice (C57BL/6; 6-8 weeks; 30-32 g; n=20) were housed in a temperature (25±1˚C) and a humidity (55±5%) and maintained under 12 h light and 12 h dark cycle with free access to food and water. All mice were purchased from Shanghai SLAC Laboratory Animals Co., Ltd. (Shanghai, China). Under intraperitoneal Zoletile® anesthesia (30 mg/kg) with xylazin (10 mg/kg), the left common carotid artery and the posterior branches of the two renal arteries were ligated to initiate cerebral aneurysms. Following the surgery, 1% normal saline was substituted for the drinking water to promote the degree of hypertension. The mice were divided into a control group with no surgery (n=10) and an aneurysm group (n=10) with ligation on the left common carotid artery and the posterior branches of the two renal arteries. The Institutional Animal Care and Use Committee of the Affiliated Hospital of Hebei University of Engineering (Hebei, China) approved all procedures prior to the initiation of the study.

In order to evaluate the effect of miR-29a on IA, the chemically modified agomir was used to increase miRNA expression *in vivo*. miRNA agomir is a chemically modified, cholesterylated, stable miRNA mimic, and its *in vivo* delivery resulted in target silencing similar to the effects induced by the overexpression of endogenous miRNA. Agomir-29a was synthesized by Guangzhou RiboBio Co., Ltd. (Guangzhou, China). The sequence of agomir-29a is 5'-ACUGAUUUC UUUUGGUGUUCAG-3'. The mice received agomir-29a (100 μl) via tail vein injection (40 mg/kg body weight; n=10) for 3 consecutive days. The mice in the no surgery group (n=10) and the aneurysm group (n=10) with ligation were treated as mentioned above. Expression of miR-29a was detected by reverse transcription-quantitative polymerase chain reaction (RT-qPCR; data not shown). At 200 days following the induction procedure, all mice were euthanized with CO gas. Cerebral arteries were dissected and stripped from brains under a surgical microscope. Samples from the regions of aneurysmal dilation on left posterior communicating artery in the aneurysm group and samples from the circles of Willis in the control groups were obtained.

Cell cultures. Human brain VSMCs (HBVSMCs; cat. no. CSC-7824W) were purchased from Creative Bioarray (Shirley, NY, USA). 293-T cells were purchased from the Type Culture Collection of the Chinese Academy of Sciences (Shanghai, China). All cells were cultured in Dulbecco's modified Eagle medium supplemented with 10% fetal bovine serum, which were purchased from Gibco (Thermo Fisher Scientific, Inc., Waltham, MA, USA) and 1% penicillin (100 U/l) and streptomycin (100 μg/ml). Cells were maintained at 37˚C in a humidified atmosphere with 5% CO_2. Cells were seeded at $10x10^6$ cells/dish in ten 15-cm dishes 1 day prior to transfection. The miR-29a mimics, miR-29a inhibitor, and the corresponding controls [mimics negative control (NC) or inhibitor NC] were obtained from GeneCopoeia, Inc. (Rockville, MD, USA). Transfection was performed using Lipofectamine® 2000 (Invitrogen; Thermo Fisher Scientific, Inc.) according to the manufacturer's protocol.

Cells were transfected with 50 nM miR-29a mimics, miR-29a inhibitor or corresponding controls for 2 h, followed by treatment with 200 μM H_2O_2 for 6 h, and cells were harvested at different times (24, 36 and 48 h) for subsequent experiments. Cells in the control group were treated with the same medium without H_2O_2 (blank group).

Patient samples. Written informed consent was obtained from patients, according to a protocol approved by the Ethics Committee of the Affiliated Hospital of Hebei University of Engineering. In total, 2 ml peripheral blood samples were obtained from 24 pairs of patients with IA and healthy volunteers from the Affiliated Hospital of Hebei University of Engineering (recruited from March 2014 to April 2015). Twenty-four patients met the inclusion criteria and were enrolled. Inclusion criteria (25) were as follows; age ≤70 years (1) and planned microsurgery or endovascular surgery for unruptured IA (2). Exclusion criteria (25) were as follows; preoperative intelligence quotient <80 (n=2) (1); initial modified Rankin scale ≥1 (n=1) (2); and loss to follow-up (n=3) (3). There were 28 males and 20 females, and the age range was 35-78 years.

RNA extraction. TissueLyser II (Qiagen, Inc., Valencia, CA, USA) was used to homogenize the aneurysm and control samples obtained from mice. Total RNA from tissue, cells and blood samples were isolated using TRIzol® reagent (Invitrogen; Thermo Fisher Scientific, Inc.) according to the manufacturer's protocol. Low molecular weight RNA (<200 nucleotides) was isolated from the total RNA by mirVana miRNA purification columns (Ambion; Thermo Fisher Scientific, Inc.) for microarray analysis and RT-qPCR, according to the manufacturer's protocol. RNA quality and quantity were determined using a NanoDrop 2000 spectrophotometer (NanoDrop Technologies; Thermo Fisher Scientific, Inc.).

Microarray and data analysis. Total RNA from samples from IA and sham mice (3/group) was sent to LC Sciences, LLC (Houston, TX, USA) for miRNA microarray analysis (miRCURY LNA™ miRNA Array kit; Exiqon A/S, Vedbaek, Denmark). Data were analyzed by one-way analysis of variance (ANOVA) using Tukey's multiple comparison test. Expression normalization was performed using a cyclic LOWESS method (26).

RT-qPCR. RNA was reverse transcribed to cDNA from 100 ng total RNA with a TIANScript II RT kit (Tiangen Biotech Co., Ltd., Beijing, China) at 37˚C for 1 h. qPCR was performed with miScript SYBRGreen PCR kit (Tiangen Biotech Co., Ltd.). Primer sequences were as follows: U6 forward, 5'-CTC GCTTCGGCAGCACA-3' and reverse, 5'-AACGCTTCA CGAATTTGCGT-3'; miR-29a forward, 5'-TGCGCTAGC ACCATCTGAAAT-3' and reverse, 5'-CAGTGCAGGGTC CGAGGT-3'; β-actin forward, 5'-GGGAAATCGTGCGTG ACATTAAG-3' and reverse, 5'-TGTGTTGGCGTACAG GTCTTTG-3'; caspase-3 forward, 5'-AGAGGAATGATT

GGGGGTG-3' and reverse, 5'-TTGCTAGGCAGTGGTAGC G-3'; caspase-9 forward, 5'-CGGAATCACCAATCATTA CAT-3' and reverse, 5'-AGAAACGCCCACAACTGC-3'; caspase-8 forward, 5'-CAGCATTAGGGACAGGAATC-3' and reverse, 5'-CAGTTATTCACAGTGGCCAT-3'; myeloid cell leukemia 1 (Mcl-1) forward, 5'-TGAAATCGTTGTCTC GAGTGATG-3' and reverse, 5'-TCACAATCGCCCCAG TTT-3'; and Cyt-c forward, 5'-CAGTGCCATACTGTGGAA AAGG-3' and reverse, 5'-TGACCTGTCTTTCGTCCAAAC A-3'. qPCR was performed on a StepOnePlus Real-Time PCR System (Applied Biosystems; Thermo Fisher Scientific, Inc.), with each reaction performed in triplicate. The PCR amplification protocol was as follows: An initial 95˚C for 5 min and 40 cycles of 94˚C for 15 sec; 55˚C for 30 sec; and 70˚C for 30 sec, followed by a final extension step of 72˚C for 10 min. The RT-qPCR assays were performed in triplicate and the alteration in expression level was normalized to the expression of U6 using the $2^{-\Delta\Delta Cq}$ method (27).

Bioinformatics TargetScan 7.0 (http://www.targetscan.org/) (28) and miRanda (http://www.microrna.org/) (29) target gene prediction software selected Mcl-1 as a target gene of miR-29a.

Terminal deoxynucleotidyl transferase-mediated bio-dUTP nick-end labelling (TUNEL) apoptosis analysis of vascular tissues from sham and IA mice. For TUNEL analysis of mouse vascular tissues, the Roche *In Situ* Cell Death Fluorescein Detection kit (Roche Diagnostics, Basel, Switzerland) was used, according to the manufacturer's protocol. Vascular tissues were fixed in 4% paraformaldehyde for 3 h at 4˚C, paraffin embedded and cut into 4 μm-thick sections. Tissue sections were subsequently de-waxed in xylene, rehydrated in graded alcohols, and placed in dH_2O. The slides were incubated for 15 min at room temperature with 20 μg/ml Proteinase K (Gibco BRL; Thermo Fisher Scientific, Inc.). The slides were rinsed twice with PBS prior to incubation in TUNEL reaction mixture for 60 min at 37˚C. The Nucleotide Mix was on ice and sufficient rTdT incubation buffer was prepared for all experimental reactions, 50 μl rTdT incubation buffer was added to each slide. The sections were covered with plastic coverslips to ensure even distribution of the reagent. The DNA fragments were labeled with the rTdT at 37˚C for 1 h in the dark. The sections were stained with 10 nM DAPI (Beyotime Institute of Biotechnology, Shanghai, China) at 37˚C for 3 min and observed using an inverted fluorescence microscope (Olympus 1X51; Olympus Corporation, Tokyo, Japan; magnification, x100; number of fields, n=5/tissue). TUNEL-positive cells were counted using ImageJ software version 1.33-1.34 (http://rsbweb.nih.gov/ij/; National Institutes of Health, Bethesda, MD, USA) for subsequent statistical analysis.

Luciferase reporter assay. miR-29a mimics, miR-29a inhibitors and negative control (NC) miRs (mimics NC and inhibitor NC) were purchased from Shanghai GenePharma Co., Ltd. (Shanghai, China). The sequences are as follows: miR-29a mimics, 5'-TAGCACCATCTGAAATCGGTTA-3'; miR-29a inhibitor, 5'-TAACCGATTTCAGATGGTGCTA-3'; mimics NC, 5'-AAATGTACTGCGCGTGGAGAC-3'; and inhibitor NC, 5'-UUCUCCGAACGUGUCACGUTT-3'. 293T cells (Type Culture Collection of the Chinese Academy of Sciences, Shanghai, China) were seeded into 48-well plates ($2x10^5$ /well) and cotransfected with miR-29a mimics/inhibitors/NC miRs (50 nM) and NFAT luciferase reporter plasmids (200 ng; Promega Corporation, Madison, WI, USA) containing a wild-type or mutant type of the Mcl-1 3' untranslated region (3'-UTR) using Lipofectamine® 2000 reagent (Invitrogen; Thermo Fisher Scientific, Inc.). At 48 h following transfection, luciferase activities were measured using the Dual-Luciferase Reporter Assay System (Promega Corporation, Madison, WI, USA). Firefly luciferase activity was normalized to the activity of *Renilla* luciferase. Each transfection was performed in triplicate.

Western blot analysis. Cells were lysed using radioimmunoprecipitation buffer (cat. no. 211-40; AmyJet Scientific, Inc., Wuhan, China). Total cell protein was extracted from cells or tissues. According to the manufacturer's protocol, the protein concentration was determined by a bicinchoninic acid protein assay kit (Beyotime Institute of Biotechnology, Haimen, China). A total of 2 μg per lane protein was electrophoresed with 10% SDS-PAGE. Subsequently, proteins were transferred onto polyvinylidene difluoride membranes (Bio-Rad Laboratories, Inc., Hercules, CA, USA) and blocked with 5% skimmed milk at room temperature for 1 h. Following blocking with milk, the membranes were incubated with specific primary antibodies at 37˚C for 2 h. β-actin was used as the internal reference. The secondary antibody (1:10,000) was added to the membrane and incubated for 1 h with agitation at room temperature. Rabbit anti-cytochrome c (Cyt-c; 1:1,000; cat. no. 4280) and anti-caspase-3 (caspase-3; cat. no. 9665; 1:1,500) were purchased from Cell Signaling Technology, Inc. (Danvers, MA, USA). Rabbit anti-Mcl-1 antibody (Mcl-1; 1:1,000; cat. no. sc-819) and anti-β-actin (1:1,500; cat. no. sc-8432) were purchased from Santa Cruz Biotechnology, Inc. (Dallas, TX, USA). The secondary antibodies included horseradish peroxidase (HRP)-conjugated goat anti-rabbit immunoglobulin G (1:2,000; cat. no. sc-2004) were purchased from Santa Cruz Biotechnology, Inc. The signals were visualized using Immobilon Western Chemiluminescent HRP Substrate (EMD Millipore, Billerica, MA, USA) and autoradiography. Densitometric levels of protein signals were quantified and presented as their ratio to β-actin. Autoradiograms were quantified by densitometry using Quantity One software version 4.4.0 (Bio-Rad Laboratories, Inc.).

Cell viability determined using an MTT assay. Cells ($5x10^5$) were seeded on 96-well plates following trypsin digestion and cell counting, and five wells in a row were used for each sample. Cells were incubated at 37˚C with 5% CO_2 for 5 days. An MTT stain was performed, according to the manufacturer's protocol. Formazan was dissolved by dimethyl sulfoxide. A microplate reader was used to measure the optical density 450 value of solution.

Apoptosis assay. A total of $10x10^4$ HBVSMCs transfected with NC miRs, miR-29a mimics and miR-29a inhibitors, were harvested by trypsinization at 48 h following transfection. An Annexin V-Fluorescein Isothiocyanate kit (BD Biosciences, San Jose, CA, USA) was used to detect apoptotic cells, according to

the manufacturer's protocol. The cells were analyzed with a flow cytometer (FACScan; BD Biosciences) equipped with CellQuest software (version 5.1; BD Biosciences). The relative ratio of early apoptotic cells was compared with control transfection from each experiment. Each sample was run in triplicate.

Statistical analysis. Data are presented as the mean ± standard deviation from at least three separate experiments. All experiments were repeated for at least three times with triplicated samples in each experiment. One-way ANOVA using Tukey's multiple comparison test was employed to evaluate the statistical differences among different groups with SPSS version 19.0 software (IBM Corp., Armonk, NY, USA). $P<0.05$ was considered to indicate a statistically significant difference.

Results

Genes and proteins involved in mitochondrial apoptosis pathways are upregulated in IA mice compared with sham controls. The activation of caspase-3, -8 and -9, which are apoptotic caspases, may serve a vital role in the process of mitochondrial apoptosis. In the present study, the mRNA expression of caspases, including caspase-3, -8 and -9, was analyzed in sham control and IA mice samples by RT-qPCR. The results demonstrated that the expression levels of caspase-3, caspase-8 and caspase-9 were significantly upregulated in the IA group compared with sham controls ($P<0.01$; Fig. 1A), which indicate that increased apoptosis occurred in IA.

To further detect whether the mitochondrial pathway is involved in the apoptosis observed in IA mice, the protein expression of Cyt-c and Mcl-1 was detected by western blotting. The results demonstrated that the protein expression of Cyt-c was activated, while Mcl-1 expression was decreased, in the IA group compared with the sham controls (Fig. 1B). Additionally, pathological analysis demonstrated that the apoptosis of VSMCs, accompanied with decreased numbers of VSMCs, occurred in the IA group (Fig. 1C). The apoptosis of vascular tissue between the two groups was detected by a TUNEL assay (Fig. 1C). Quantification of TUNEL staining demonstrated that apoptosis was significantly increased in the IA group compared with the sham group ($P<0.01$). These results indicated that mitochondrial apoptosis may participate in the process of IA.

Expression profiles of miRNAs in IAs and sham control arteries. miRNAs have been reported to regulate the mitochondrial apoptosis pathway (30,31). In the present study, to detect the miRNAs that may be involved in the IA process, an miRNA array was used. Significantly different expression levels of miRNAs were identified between the IA group and the sham controls, with 31 miRNAs significantly upregulated and 20 miRNAs significantly downregulated (fold change value >2; $P<0.05$) in the IA tissues compared with the control group (Fig. 2A).

For validation of the microarray data, the most dysregulated miRs, including miR-29a, miR-233, miR-433, miR-489 and miR-126 were selected for RT-qPCR analysis. The relative expression alterations of these miRNA analyzed by RT-qPCR were consistent with the microarray analysis results, with the exception of miR-126, which was not significantly altered between the sham control and IA mice ($P<0.05$; Fig. 2B). In order to determine whether miR-29a expression in IA mice models exhibits a similar pattern to clinical patients, a clinical experiment was performed to detect miR-29a expression in patients with IA and healthy volunteers. The blood samples obtained from the case group included 24 patients with IA, while the control group included 24 healthy volunteers. miR-29a expression was detected and compared between the two groups. The results of RT-qPCR demonstrated that the expression of miR-29a in patients with IA was significantly higher compared with healthy controls ($P<0.01$; Fig. 2C).

miR-29a has been reported as a potential biomarker in the development of IA (31). In addition, it has been reported that upregulation of miR-29a may be implicated in cell apoptosis by targeting Mcl-1 expression in rat germ cell death (32). Previous studies have demonstrated that miR-29a is able to induce cell apoptosis by activating caspase proteins (33,34). For example, miR-29a was reported to be responsible for the activation of caspase-3-induced K562 cell apoptosis (35). Therefore, miR-29a was selected for further investigation in the present study.

miR-29a downregulation inhibits the apoptosis of HBVSMCs. An *in vitro* H_2O_2-induced apoptosis model was established to mimic IA (36). HBVSMCs were treated with H_2O_2 (0-300 μM) and miR-29a expression levels were significantly increased in a concentration-dependent manner, peaking at 200 μM, compared with the 0 μM group (Fig. 2D). Based on these results, the concentration of 200 μM H_2O_2 was selected for subsequent experiments.

HBVSMC cells were transfected with miR-29a mimics or inhibitor. Fig. 3A demonstrates that the expression of miR-29a was significantly upregulated in the miR-29a mimic treatment group compared with the mimics NC group ($P<0.01$), while miR-29a expression was significantly decreased in cells with miR-29a inhibitor treatment compared with the inhibitor NC group ($P<0.01$). Following transfection with miR-29a inhibitor for 24, 36 and 48 h, the cell viability of VSMCs treated with H_2O_2 was significantly increased, compared with the inhibitor NC treatment group ($P<0.01$; Fig. 3B). However, the H_2O_2-induced reduction of HBVSMC viability was significantly enhanced following transfection with miR-29a mimics, compared with the mimics NC treatment group ($P<0.01$; Fig. 3C). These results indicated that the miR-29a inhibitor reversed H_2O_2-induced cell viability inhibition, while miR-29a mimics promoted H_2O_2-induced cell viability inhibition.

Furthermore, treatment with 200 μM H_2O_2 indicated that transfection of miR-29a inhibitor protected against H_2O_2-induced HBVSMC apoptosis, while miR-29a mimics worsened the H_2O_2-induced HBVSMC apoptosis ($P<0.05$; Fig. 3D and E). Western blot analysis was performed to observe alterations in the protein expression of apoptosis-associated proteins in H_2O_2-induced HBVSMCs transfected with miR-29a inhibitor or mimics. In H_2O_2-treated cells with miR-29a inhibitor treatment, the expression levels of the proapoptotic proteins caspase-3 and Cyt-c were decreased, while Mcl-1 was increased, compared with the inhibitor NC group ($P<0.01$; Fig. 3F). Conversely, in cells treated with miR-29a mimics, the expression levels of the proapoptotic proteins caspase-3 and Cyt-c were increased, while Mcl-1 was decreased, compared

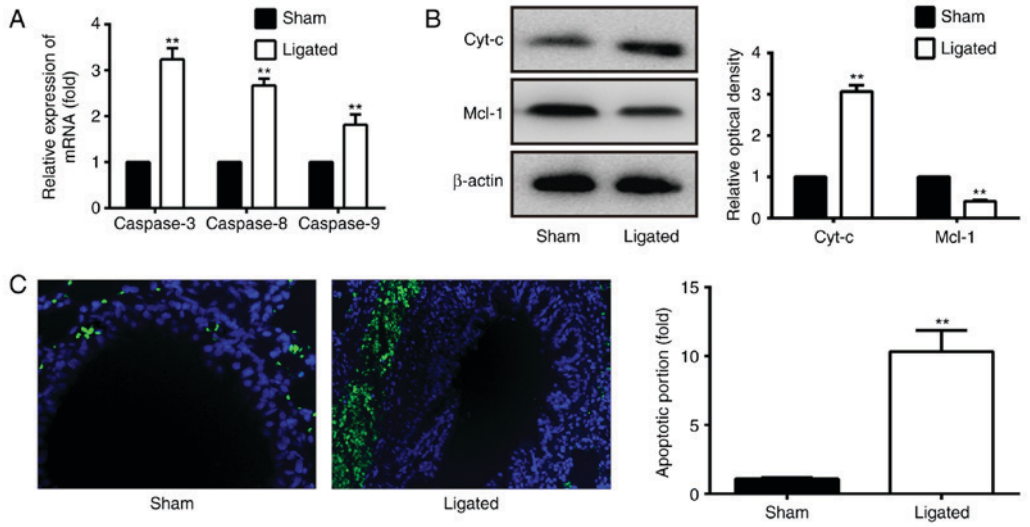

Figure 1. Genes and proteins involved in mitochondrial apoptosis pathways are upregulated in IA mice compared with sham controls. (A) mRNA expression of caspases was analyzed in sham control and IA mouse samples by reverse transcription-quantitative polymerase chain reaction. The mRNA expression of caspase-3, -8 and -9 was significantly upregulated in the IA group compared with sham controls. (B) Protein expression of Cyt-c and Mcl-1 was detected in IA and sham control mice by western blotting. Cyt-c expression was significantly increased, while Mcl-1 was significantly decreased, in the IA group when compared with the sham controls. (C) Apoptosis of vascular tissue between the two groups was detected by terminal deoxynucleotidyl transferase-mediated bio-dUTP nick-end labelling assay (magnification, x200). **P<0.01 vs. sham group. IA, intracranial aneurysm; Cyt-c, cytochrome c; Mcl-1, myeloid cell leukemia 1; ligated, IA group.

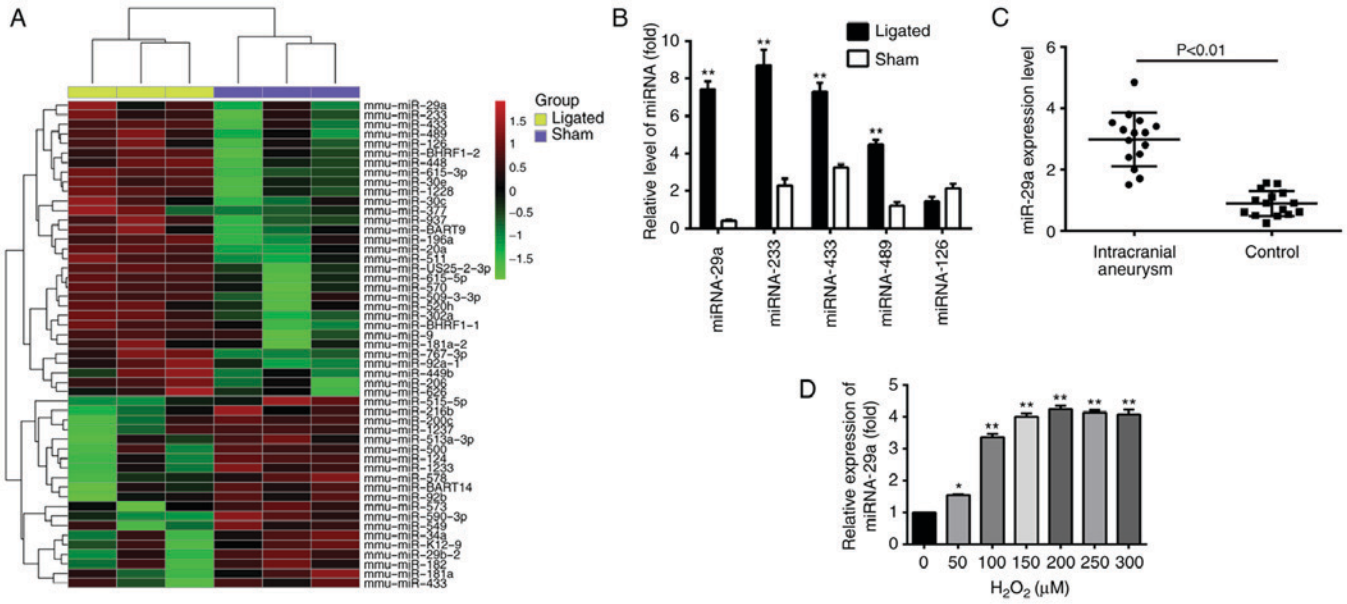

Figure 2. Hierarchical clustering analysis of miRNA expression in the cerebral arteries of IA and sham control mice. (A) Hierarchical clustering analysis of miRNAs that were significantly downregulated or upregulated in IA mice compared with sham controls. miRNAs are presented in rows and samples are presented in columns. Colors indicate the relative signal intensities, where red and green colors indicate upregulated and downregulated miRNAs, respectively. (B) miR-29a, miR-233, miR-433, miR-489 and miR-126 were selected to validate the microarray analysis data by RT-qPCR analysis. Relative expression levels are plotted on the y-axis. **P<0.01 vs. sham group. (C) miR-29a expression in blood samples from patients with IA and healthy volunteers was detected by RT-qPCR analysis. (D) miR-29a expression levels in human brain vascular smooth muscle cells treated with different concentrations of H_2O_2 were measured by RT-qPCR. *P<0.05 and **P<0.01 vs. 0 μM H_2O_2. miRNA/miR, microRNA; IA, intracranial aneurysm; RT-qPCR, reverse transcription-quantitative polymerase chain reaction; ligated, IA group.

with the mimics NC group (P<0.01; Fig. 3G). These results indicated that miR-29a may regulate cell apoptosis during IA.

miR-29a directly targets Mcl-1. miR-29a has been reported to directly target Mcl-1 in intestinal epithelial cells (37). In the present study, bioinformatics tools, TargetScan and miRanda, were used to identify the target genes of miR-29a. Fig. 4A demonstrates that Mcl-1 is a theoretical target gene of miR-29a. The wild-type 3'-UTR of the Mcl-1 gene was cloned and inserted it into the downstream region of a luciferase reporter gene. Subsequently, miR-29a mimics/inhibitors were cotransfected with different luciferase 3'-UTR constructs into 293T cells. The results of luciferase assays demonstrated that miR-29a mimics significantly weakened the relative

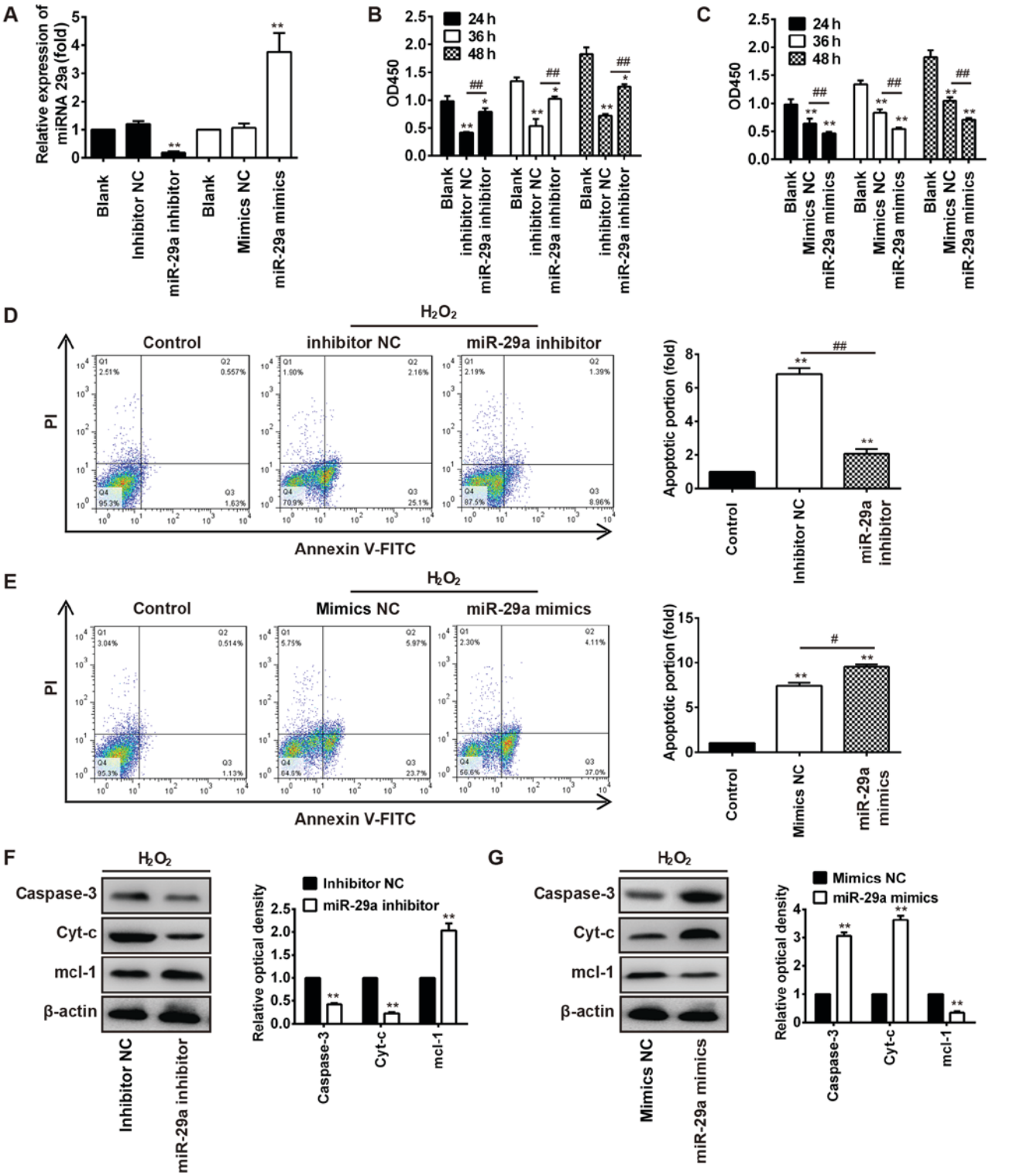

Figure 3. miR-29a inhibition protects HBVSMCs against H_2O_2-induced apoptosis. (A) miR-29a expression was detected by reverse transcription-quantitative polymerase chain reaction in HBVSMCs treated with miR-29a mimics or miR-29a inhibitor. **P<0.01 vs. inhibitor NC or mimics NC group. (B) Cell viability was analyzed using a Cell Counting kit-8 assay. The OD 450 values were detected by using a SpectraMax microplate reader. miR-29a inhibitor reversed H_2O_2-induced cell viability inhibition in a time-dependent manner in HBVSMCs. *P<0.05, **P<0.01 vs. Blank group; $^{\#\#}$P<0.01 vs. inhibitor NC group. (C) Transfection of miR-29a mimics enhanced H_2O_2-induced cell viability inhibition in HBVSMCs. **P<0.01 vs. Blank group, $^{\#\#}$P<0.01 vs. mimics NC group. (D) Apoptotic cells were detected by Annexin V-FITC and PI apoptosis detection kit, and were analyzed with a flow cytometer. Treatment with miR-29a inhibitor protected HBVSMCs from H_2O_2-induced apoptosis. Cells in the lower left quadrant represent intact viable cells (Annexin negative and PI negative), cells in the lower right quadrant represent early apoptotic cells (Annexin positive and PI negative), cells in the upper right quadrant represent late apoptotic cells (Annexin positive and PI positive) and cells in the upper left quadrant represent necrotic cells (Annexin negative and PI positive). **P<0.01 vs. blank group; $^{\#\#}$P<0.01, as indicated. (E) miR-29a mimic treatment enhanced the H_2O_2-induced apoptosis of HBVSMCs. **P<0.01 vs. blank group; $^{\#}$P<0.05, as indicated. (F) Western blotting results demonstrated that the protein levels of caspase-3 and Cyt-c were significantly reduced following miR-29a inhibitor transfection, while anti-apoptosis protein Mcl-1 expression was increased. **P<0.01 vs. inhibitor NC group. (G) Western blotting results demonstrated that the protein levels of the pro-apoptosis proteins, caspase-3 and Cyt-c, were significantly increased following miR-29a mimics transfection, while anti-apoptosis protein Mcl-1 expression was decreased. **P<0.01 vs. mimics NC group. miR, microRNA; HBVSMCs, human brain vascular smooth muscle cells; NC, negative control; OD, optical density; PI, propidium iodide; Cyt-c, cytochrome c; Mcl-1, myeloid cell leukemia 1; FITC, fluorescein isothiocyanate.

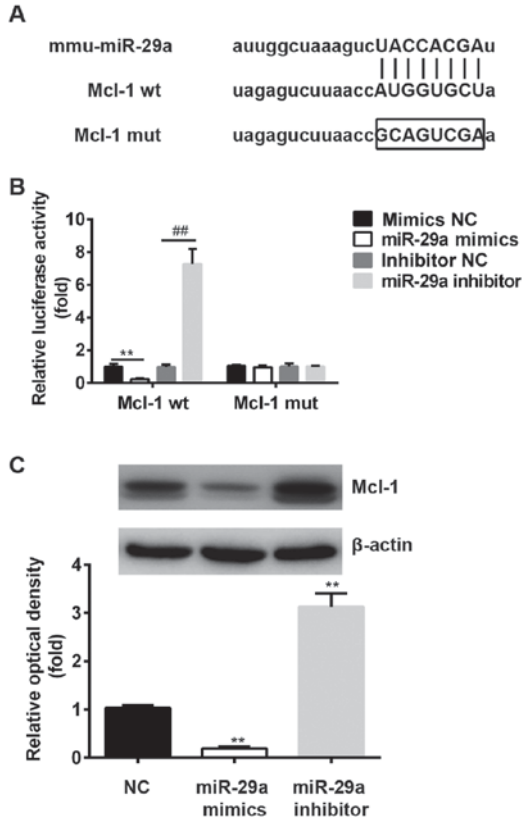

Figure 4. miR-29a directly targets the Mcl-1 gene. (A) A putative miR-29a-binding site exists in the 3'-UTR of Mcl-1 mRNA and point mutations were generated in the binding site. (B) Luciferase reporter plasmid containing wild-type or mutant Mcl-1 3'-UTR was cotransfected into 293T cells with miR-29a mimic/inhibitor or NC miRs. Luciferase activity was determined by the Dual-Luciferase Reporter Assay System and presented as the relative firefly luciferase activity normalized to *Renilla* activity. Each bar represents the mean + standard deviation of three independent experiments. **P<0.01; $^{\#\#}$P<0.01. (C) Protein expression of Mcl-1 in human brain vascular smooth muscle cells was detected by western blotting following treatment with miR-29a mimics or miR-29a inhibitor (n=3). P<0.01 vs. NC. miR, microRNA; myeloid cell leukemia 1; 3'-UTR', 3'-untranslated region; NC, negative control; wt, wild-type; mut, mutant.

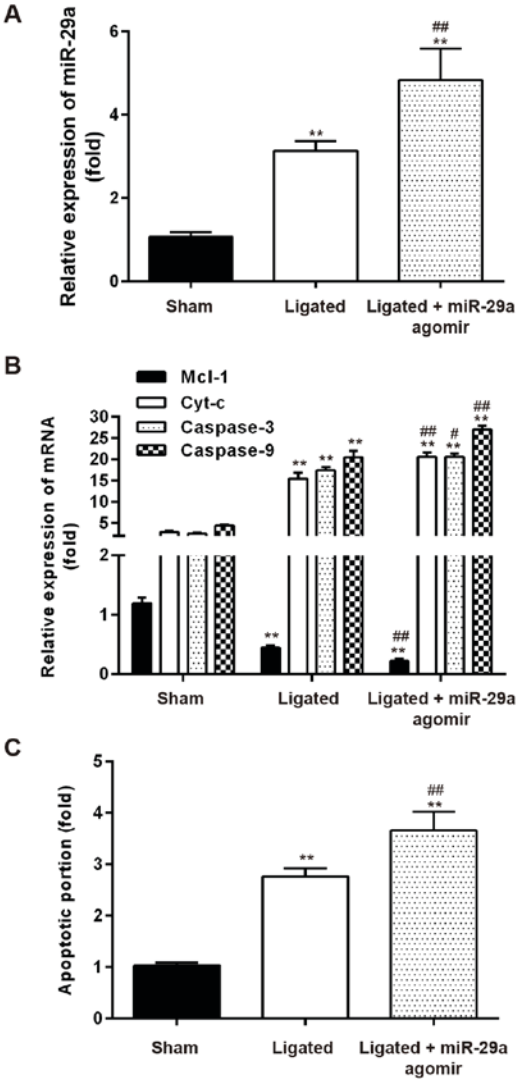

Figure 5. miR-29a contributes to IA progression by regulating the mitochondrial apoptotic pathway in mouse models. (A) Quantitative reverse transcription-polymerase chain reaction analysis was used to detect the expression of miR-29a between groups. (B) Relative mRNA expression of Mcl-1, Cyt-c, caspase-3 and caspase-9 in sham-operated mice, IA ligated mice and IA + agomir-miR-29a mice (n=10/group) was determined by reverse transcription-quantitative polymerase chain reaction. (C) Terminal deoxynucleotidyl transferase-mediated bio-dUTP nick-end labelling confirmed that apoptosis in tissue sections was significantly increased in IA + agomir-miR-29a mice compared with the IA ligated mice. Results are presented as the mean + standard deviation. n=10/group. **P<0.01 vs. sham group; $^{\#}$P<0.05, $^{\#\#}$P<0.01 vs. ligated group. miR, microRNA; IA, intracranial aneurysm; Mcl-1, myeloid cell leukemia 1; Cyt-c, cytochrome c; ligated, IA group.

luciferase activity of the luciferase reporter containing the wild-type 3'-UTR of Mcl-1 mRNA compared with mimics NC group, whereas the knockdown of miR-29a increased luciferase activity (P<0.01; Fig. 4B). To determine whether Mcl-1 mRNA is directly targeted by miR-29a, the predicted binding site of miR-29a in the 3'-UTR of Mcl-1 was muted. By contrast, the luciferase activities of luciferase reporters containing mutant 3'-UTRs of Mcl-1 luciferase activity remained unaltered in miR-29a mimic/inhibitor-transfected 293T cells compared with the respective mimics/inhibitor NC groups (Fig. 4B).

Results from the western blot analysis demonstrated that the protein expression of Mcl-1 was markedly decreased following miR-29a mimic treatment and increased following miR-29a inhibitor treatment, compared with the NC group (Fig. 4C).

Overexpression of miR-29a promotes apoptosis in vivo. As miR-29a overexpression *in vitro* enhanced VHBSMC apoptosis (Fig. 3B) and Mcl-1 was determined as a direct target of miR-29a (Fig. 4), the present study aimed to determine whether miR-29a may regulate apoptosis by regulating Mcl-1 expression *in vivo*. The miR-29a function in IA injury was detected by administration of the agomir-miR-29a to mice. As demonstrated in Fig. 5A, the expression of miR-29a in IA ligated mice was significantly higher compared with sham mice, while the level of miR-29a is further significantly increased in agomir-miR-29a + IA ligated mice. RT-qPCR results demonstrated that genes involved in mitochondrial apoptosis pathways, including Cyt-c, caspase-3 and caspase-9, were markedly increased, while Mcl-1 was decreased, in the IA ligated mice compared with sham controls (Fig. 5B). In agomir-miR-29a + IA ligated mice, Cyt-c, caspase-3 and caspase-9 were significantly increased, while the anti-apoptosis

gene Mcl-1 was decreased, compared with the IA ligated group (Fig. 5B), indicating that miR-29a overexpression promoted mitochondrial apoptosis *in vivo*. TUNEL staining confirmed that apoptosis in tissue sections was significantly increased in IA + miR-29a agomir mice, compared with IA ligated mice ($P<0.01$; Fig. 5C).

Taken together, these results indicated that miR-29a overexpression may stimulate mitochondrial apoptosis pathways, subsequently contributing to the injury caused by IA.

Discussion

The development and growth of aneurysms involve the complex events of arterial wall cells remodeling (38). Previous studies have demonstrated that apoptosis is involved in the pathogenesis of aneurysms (6,7). However, the molecular mechanisms underlying the stimulation of apoptosis in the mouse IA model remains unknown.

To investigate the apoptotic events of IA mice model, the present study investigated the mRNA expression of caspases associated with the mitochondrial apoptotic pathway, including caspase-3, -8 and -9. The activation of caspases serves an essential role during the process of apoptosis (39), which may be caused by an extrinsic or intrinsic pathway, which lead to a terminal common pathway (40). Caspase-8 activation is involved in the extrinsic pathway and caspase-9 is involved in the intrinsic pathway. In the mitochondrial pathway, the release of Cyt-c constitutes an apoptotic complex, which subsequently results in the activation of caspase-9. The activation of caspase-8 and -9 leads to the subsequent activation of caspase-3, which mediates cell apoptosis (11). In the present study, the expression levels of the proapoptotic genes, caspase-3, -8 and -9, were markedly increased in IA mice samples, indicating that the mitochondrial pathway may be involved in apoptosis in the IA mouse model, as caspase activation serves an important function in apoptosis.

It has been confirmed that miRNAs regulate various biological events, including development, metabolism, proliferation, differentiation and apoptosis (41). Studies have demonstrated the contribution of miRNAs together with their target genes in controlling IA injury in a number of models (18,19). Therefore, to investigate the molecular mechanism of apoptosis in IA injury, the present study focused on miRNA regulation. Results from microarray analysis and RT-qPCR demonstrated that among the upregulated miRNAs in IA mice models, miR-29a demonstrated the highest upregulation level.

It has been demonstrated that miR-29a may regulate the mitochondrial apoptosis pathway and activate caspases, including caspase-3 and -8 (31). Additionally, it has been reported that miR-29a expression was significantly increased following ischemia-reperfusion (I/R) and induced apoptosis, and transfection with anti-miR-29a reduced the levels of apoptosis in cells and provided them with protection against I/R injury (42). The primary aim of the present study was to investigate whether miR-29 may be involved in IA-associated apoptosis, a key process in the pathogenesis of IA. The present study identified that mitochondrial apoptosis may occur in IA. To investigate the association between miR-29a and caspases in IA, *in vitro* experiments were performed, which demonstrated that miR-29a mimics induced the activation of caspase-3, -8 and -9. These results indicated that upregulation of miR-29a may promote the mitochondrial apoptosis pathway in IA.

Apoptosis is a parameter of IA injury. VSMCs constitute the majority of the blood vessel wall (43) and their growth or programmed cell apoptosis serves an important role in the altered geometry of vessels in vascular diseases, thus promoting the rupture of aneurysms. Accordingly, VSMC apoptosis was utilized as an *in vitro* model of IA (35). Results from the present study demonstrated that miR-29a inhibition attenuated the apoptosis of HBVSMCs; whereas, miR-29a overexpression increased HBVSMC apoptosis.

Mcl-1 is reported to be associated with the programming of differentiation and cell viability/death (44). In the present study, Mcl-1 was identified as being directly targeted by miR-29a and involved in IA-induced apoptosis, and an *in vivo* model was established to determine whether apoptosis may be regulated by miR-29a in IA. Results from the RT-qPCR and apoptosis detection analysis demonstrated that the overexpression of miR-29a significantly enhanced the mitochondrial apoptosis of IA injury, as may be inferred from the increased mRNA expression levels of genes involved in the mitochondrial pro-apoptosis pathways (caspase-3 and -8 and Cyt-c), decreased anti-apoptotic gene Mcl-1 expression and enhanced cell death by DNA fragmentation compared with the IA ligated group.

It is therefore concluded that miR-29a may contribute to the progression of IA by regulating the mitochondrial apoptotic pathways. However, further studies are required for verification of these results. Therefore, miR-29a may be a novel target for the prevention and treatment of IA.

Acknowledgements

Not applicable.

Funding

No funding was received.

Availability of data and materials

The datasets used and/or analyzed during the current study are available from the corresponding author on reasonable request.

Authors' contributions

WZ performed the experiments, contributed to data analysis and wrote the paper. J-YS analyzed the data. HZ conceptualized the study design, and contributed to data analysis and experimental materials. All authors read and approved the final manuscript.

Ethics approval and consent to participate

Experiments involving human and animal tissues were approved by the Ethics Committee of The Affiliated Hospital

of Hebei University of Engineering. Written informed consent was obtained from all human participants.

Patient consent for publication

Not applicable.

Competing interests

The authors declare that they have no competing interests.

References

1. Kacar E, Fatih Nas O, Erdogan C and Hakyemez B: Intracranial aneurysm rupture during flow diverter stent placement: Successful treatment with stent-in-stent combination. Diagn Interv Imaging 96: 411-413, 2015.
2. Komotar RJ, Zacharia BE, Otten ML, Mocco J and Lavine SD: Controversies in the endovascular management of cerebral vasospasm after intracranial aneurysm rupture and future directions for therapeutic approaches. Neurosurgery 62: 897-907, 2008.
3. Lee D, Ahn SJ, Cho ES, Kim YB, Song SW, Jung WS and Suh SH: High prevalence of intracranial aneurysms in patients with aortic dissection or aneurysm: Feasibility of extended aorta CT angiography with involvement of intracranial arteries. J Neurointerv Surg 9: 1017-1021, 2017.
4. Ronkainen A, Hernesniemi J, Ryynänen M, Puranen M and Kuivaniemi H: A ten percent prevalence of asymptomatic familial intracranial aneurysms: Preliminary report on 110 magnetic resonance angiography studies in members of 21 Finnish familial intracranial aneurysm families. Neurosurgery 35: 208-213, 1994.
5. Frösen J, Piippo A, Paetau A, Kangasniemi M, Niemelä M, Hernesniemi J and Jääskeläinen J: Remodeling of saccular cerebral artery aneurysm wall is associated with rupture: Histological analysis of 24 unruptured and 42 ruptured cases. Stroke 35: 2287-2293, 2004.
6. Guo F, Li Z, Song L, Han T, Feng Q, Guo Y, Xu J, He M and You C: Increased apoptosis and cysteinyl aspartate specific protease-3 gene expression in human intracranial aneurysm. J Clin Neurosci 14: 550-555, 2007.
7. Pentimalli L, Modesti A, Vignati A, Marchese E, Albanese A, Di Rocco F, Coletti A, Di Nardo P, Fantini C, Tirpakova B and Maira G: Role of apoptosis in intracranial aneurysm rupture. J Neurosurg 101: 1018-1025, 2004.
8. Liu CY, Su JC, Huang TT, Chu PY, Huang CT, Wang WL, Lee CH, Lau KY, Tsai WC, Yang HP, *et al*: Sorafenib analogue SC-60 induces apoptosis through the SHP-1/STAT3 pathway and enhances docetaxel cytotoxicity in triple-negative breast cancer cells. Mol Oncol 11: 266-279, 2017.
9. Apoptosis in cancer pathogenesis and anti-cancer therapy. New perspectives and opportunities. Gregory, Christopher D. (ed.). AntiCancer Res 37: 371, 2016.
10. Chen Z, Miao H, Feng H and Zhu G: Rupture of an infectious intracranial aneurysm involving two parent arteries after surgical treatment of infective endocarditis. Neurosciences (Riyadh) 16: 72-75, 2011.
11. Kadirvel R, Ding YH, Dai D, Lewis DA and Kallmes DF: Intrinsic pathway-mediated apoptosis in elastase-induced aneurysms in rabbits. AJNR Am J Neuroradiol 31: 165-169, 2010.
12. Bartel DP: MicroRNAs: Genomics, biogenesis, mechanism, and function. Cell 116: 281-297, 2004.
13. Chen B, Li H, Zeng X, Yang P, Liu X, Zhao X and Liang S: Roles of microRNA on cancer cell metabolism. J Transl Med 10: 228, 2012.
14. An YR, Kim SJ, Oh MJ, Kim HM, Shim IS, Kim PJ, Choi K and Hwang SY: Analysis of microRNA and gene expression profiling in triazole fungicide-treated HepG2 cell line. Toxicology 303: 94-98, 2013.
15. Kirigin FF, Lindstedt K, Sellars M, Ciofani M, Low SL, Jones L, Bell F, Pauli F, Bonneau R, Myers RM, *et al*: Dynamic microRNA gene transcription and processing during T cell development. J Immunol 188: 3257-3267, 2012.
16. Sessa WC: MicroRNA regulation of cardiovascular functions. Arterioscler Thromb Vasc Biol 31: 2369, 2011.
17. Cui RR, Li SJ, Liu LJ, Yi L, Liang QH, Zhu X, Liu GY, Liu Y, Wu SS, Liao XB, *et al*: MicroRNA-204 regulates vascular smooth muscle cell calcification in vitro and in vivo. Cardiovasc Res 96: 320-329, 2012.
18. Cheng Y and Zhang C: MicroRNA-21 in cardiovascular disease. J Cardiovasc Transl Res 3: 251-255, 2010.
19. Luo J, Jin H, Jiang Y, Ge H, Wang J and Li Y: Aberrant expression of microRNA-9 contributes to development of intracranial aneurysm by suppressing proliferation and reducing contractility of smooth muscle cells. Med Sci Monit 22: 4247-4253, 2016.
20. Torella D, Iaconetti C, Catalucci D, Ellison GM, Leone A, Waring CD, Bochicchio A, Vicinanza C, Aquila I, Curcio A, *et al*: MicroRNA-133 controls vascular smooth muscle cell phenotypic switch in vitro and vascular remodeling in vivo. Circ Res 109: 880-893, 2011.
21. Engelhardt S and Leierseder S: Coinciding functions for miR-145 in vascular smooth muscle and cardiac fibroblasts. J Mol Cell Cardiol 65: 105-107, 2013.
22. Rangrez AY, Massy ZA, Metzinger-Le Meuth V and Metzinger L: miR-143 and miR-145: Molecular keys to switch the phenotype of vascular smooth muscle cells. Circ Cardiovasc Genet 4: 197-205, 2011.
23. Wang GK, Zhu JQ, Zhang JT, Li Q, Li Y, He J, Qin YW and Jing Q: Circulating microRNA: A novel potential biomarker for early diagnosis of acute myocardial infarction in humans. Eur Heart J 31: 659-666, 2010.
24. Wu X, Zhang J, Huang Q, Yang P, Chen J and Liu J: MicroRNA-92a regulates expression of kruppel-like factor2 in rabbit model of intracranial aneurysm. Cell Mol Biol (Noisy-le-grand) 61: 44-48, 2015.
25. Wardlaw JM and White PM: The detection and management of unruptured intracranial aneurysms. Brain 123: 205-221, 2000.
26. Bolstad BM, Irizarry RA, Astrand M and Speed TP: A comparison of normalization methods for high density oligonucleotide array data based on variance and bias. Bioinformatics 19: 185-193, 2003.
27. Livak KJ and Schmittgen TD: Analysis of relative gene expression data using real-time quantitative PCR and the 2(-Delta Delta C(T)) method. Methods 25: 402-408, 2001.
28. Friedman RC, Farh KK, Burge CB and Bartel DP: Most mammalian mRNAs are conserved targets of microRNAs. Genome Res 19: 92-105, 2009.
29. Betel D, Wilson M, Gabow A, Marks DS and Sander C: The microRNA.org resource: Targets and expression. Nucleic Acids Res 36 (Database Issue): D149-D153, 2008.
30. Zeng CW, Zhang XJ, Lin KY, Ye H, Feng SY, Zhang H and Chen YQ: Camptothecin induces apoptosis in cancer cells via microRNA-125b-mediated mitochondrial pathways. Mol Pharmacol 81: 578-586, 2012.
31. Wang WH, Wang YH, Zheng LL, Li XW, Hao F and Guo D: MicroRNA-29a: A potential biomarker in the development of intracranial aneurysm. J Neurol Sci 364: 84-89, 2016.
32. Meunier L, Siddeek B, Vega A, Lakhdari N, Inoubli L, Bellon RP, Lemaire G, Mauduit C and Benahmed M: Perinatal programming of adult rat germ cell death after exposure to xenoestrogens: Role of microRNA miR-29 family in the down-regulation of DNA methyltransferases and Mcl-1. Endocrinology 153: 1936-1947, 2012.
33. Li MN, Li SS, Meng FS, Han P, Zhang WH, Zhang LB: Mechanism and influence of down-regulation of miR-29a-3p expression on apoptosis in mouse macrophage. J South China Agricult Univ 39: 64-69, 2018.
34. Khamisipour G, Mansourabadi E, Naeimi B, Moazzeni A, Tahmasebi R, Hasanpour M, Mohammadi MM, Mansourabadi Z and Shamsian S: Knockdown of microRNA-29a regulates the expression of apoptosis-related genes in MCF-7 breast carcinoma cells. Mol Clin Oncol 8: 362-369, 2018.
35. Wang X, Zhong H, Wang L, Dong Y, Jia A, Mo Q and Zhang C: MiR-29 induces K562 cell apoptosis by down-regulating FoxM1. Med Sci Monit 21: 3115-3120, 2015.
36. Wu L, Li X, Li Y, Wang L, Tang Y and Xue M: Proliferative inhibition of danxiongfang and its active ingredients on rat vascular smooth muscle cell and protective effect on the VSMC damage induced by hydrogen peroxide. J Ethnopharmacol 126: 197-206, 2009.
37. Lv B, Liu Z, Wang S, Liu F, Yang X, Hou J, Hou Z and Chen B: MiR-29a promotes intestinal epithelial apoptosis in ulcerative colitis by down-regulating Mcl-1. Int J Clin Exp Pathol 7: 8542-8552, 2014.

38. Laine MT, Björck M, Beiles CB, Szeberin Z, Thomson I, Altreuther M, Debus ES, Mani K, Menyhei G and Venermo M: Few internal iliac artery aneurysms rupture under 4 cm. J Vasc Surg 65: 76-81, 2017.
39. Piao L, Canguo Z, Wenjie L, Xiaoli C, Wenli S and Li L: Lipopolysaccharides-stimulated macrophage products enhance Withaferin A-induced apoptosis via activation of caspases and inhibition of NF-κB pathway in human cancer cells. Mol Immunol 81: 92-101, 2017.
40. Chang JP, Chen MC, Liu WH, Lin YS, Huang YK, Pan KL, Ho WC, Fang CY, Chen CJ and Chen HC: Mitochondrial apoptotic pathway activation in the atria of heart failure patients due to mitral and tricuspid regurgitation. Exp Mol Pathol 99: 65-73, 2015.
41. Zandberga E, Kozirovskis V, Ābols A, Andrējeva D, Purkalne G and Linē A: Cell-free microRNAs as diagnostic, prognostic, and predictive biomarkers for lung cancer. Genes Chromosomes Cancer 52: 356-369, 2013.
42. Wang L, Niu X, Hu J, Xing H, Sun M, Wang J, Jian Q and Yang H: After myocardial ischemia-reperfusion, miR-29a, and Let7 could affect apoptosis through regulating IGF-1. Biomed Res Int 2015: 245412, 2015.
43. Xu F, Ahmed AS, Kang X, Hu G, Liu F, Zhang W and Zhou J: MicroRNA-15b/16 attenuates vascular neointima formation by promoting the contractile phenotype of vascular smooth muscle through targeting YAP. Arterioscler Thromb Vasc Biol 35: 2145-2152, 2015.
44. Yang T, Buchan HL, Townsend KJ and Craig RW: MCL-1, a member of the BLC-2 family, is induced rapidly in response to signals for cell differentiation or death, but not to signals for cell proliferation. J Cell Physiol 166: 523-536, 1996.